Electronic Supplementary Information accompanying:

Observations of tetrel bonding between sp^3–carbon and THF

V. L. Heywood,[a] T. P. J. Alford,[a] J. J. Roeleveld,[b] S. J. Lekanne Deprez,[b] A. Verhoofstad,[b] J. I. van der Vlugt,[b,c] S. R. Domingos,[d] M. Schnell,[d,e] A. P. Davis[a] and T. J. Mooibroek[b,*]

[a] School of Chemistry, University of Bristol, Cantock's Close, Bristol, BS8 1TS, United Kingdom. [b] van 't Hoff Institute for Molecular Sciences, Universiteit van Amsterdam, Science Park 904, 1098 XH Amsterdam, The Netherlands. [c] Institute of Chemistry, Carl von Ossietzky University Oldenburg, Carl von Ossietzky-Straße 9-11, D-26211 Oldenburg, Germany. [d] Deutsches Elektronen-Synchrotron DESY, Notkestraße 85, 22607 Hamburg, Germany. [e] Institut für Physikalische Chemie, Christian-Albrechts-Universität zu Kiel, Max-Eyth-Str.1, 24118 Kiel, Germany.

* contact: t.j.mooibroek@uva.nl

Contents:

Materials and methods

All commercially available chemicals were purchased from Sigma-Aldrich and used without further purification. Solvents were utilized as supplied.

^{1}H-, ^{13}C-, and 2D-NMR spectra were acquired at 298 K on a Varian VNMR S500a. Chemical shifts (δ) are reported in parts per million (p.p.m.). Residual solvent resonances were used as internal reference for δ-values in ^{1}H-, and ^{13}C-NMR.

The FT-IR spectrum was measured on a A Shimadzu MIRacle 10 single reflection ATR with IRAffinity-1S Fourier transform infrared spectrophotometer.

C, H, N elemental composition was analysed at the Microanalytical laboratory of the University of Bristol.

Field desorption (FR+eiFi)) mass spectra were recorded on an Advion (T)LC-MS expression LCMS mass spectrometer (with a TLC plate express and isocratic pump).

CryoSpray Ionization High Resolution Mass Spectrometry (CSI HRMS) was conducted on a HR-ToF Bruker Daltonik GmbH (Bremen, Germany) Impact II, an ESI-ToF MS capable of resolution of at least 40000 FWHM, which was coupled to a Bruker cryo-spray unit. Detection was in negative-ion mode and the source voltage was between 4 and 6 kV. The sample was introduced with a syringe pump at a flow rate of 18 ul/hr. The drying gas (N_2) was held at -35 °C and the spray gas was held at -40 °C. The machine was calibrated prior to every experiment via direct infusion of a TFA-Na solution, which provided a m/z range of singly charged peaks up to 3500 Da in both ion modes. Software acquisition Compass 2.0 for Otof series. Software processing Compass DataAnalysis 4.0 sri (x64). Both Bruker Daltonik GmbH (Bremen, Germany).

X-ray intensities were measured on a Bruker D8 Quest Eco diffractometer equipped with a Triumph monochromator (λ = 0.71073 Å) and a CMOS Photon 50 detector at a temperature of 150(2) K. Intensity data were integrated with the Bruker APEX2 software.[1] Absorption correction and scaling was performed with SADABS.[2] The structures were solved using intrinsic phasing with the program SHELXT.[1] Least-squares refinement was performed with SHELXL-2013[3] against F^2 of all reflections. Non-hydrogen atoms were refined with anisotropic displacement parameters. The H atoms were placed at calculated positions using the instructions AFIX 13, AFIX 43 or AFIX 137 with isotropic displacement parameters having values 1.2 or 1.5 times *U*eq of the attached C atoms. CCDC 1983293 contain the supplementary crystallographic data for this paper. These data can be obtained free of charge from The Cambridge Crystallographic Data Centre via www.ccdc.cam.ac.uk/data_ request/cif.

DFT geometry optimization calculations were performed with Spartan 2016 at the B3LYP[4, 5]-D3[6]/def2-TZVP[7, 8] level of theory, which is known to give accurate results at reasonable computational cost and a very low basis set superposition error (BSSE).[6-8] The molecular fragments were manually oriented in a suitable orientation before starting an unconstrained geometry optimization. The Amsterdam Density Functional (ADF)[9] modelling suite at the B3LYP[4, 5]-D3[6]/TZ2P[7, 8] level of theory (no frozen cores) was used for energy decomposition and 'atoms in molecules'[10] analyses. Details of the Morokuma-Ziegler inspired energy decomposition scheme used in the ADF-suite have been reported elsewhere[9, 11] and the scheme has proven useful to evaluate hydrogen bonding interactions.[12, 13]

Chirped Pulse Fourier Transform Microwave (CP-FTMW) Spectroscopy was conducted on the COMPACT[14, 15] spectrometer in Hamburg. A supersonic expansion brings the sample into the vacuum chamber where a 4 μs chirp spanning 2-8 GHz polarizes the ensemble of molecules. The cold molecular jet is generated using a pulsed nozzle (Parker General Valve Series 9) operating at 9 Hz with a constant flow of Ne at stagnation

pressure of 1.5 bar. To create sufficient vapour pressure a sample of **1** was heated to 180 °C directly at the nozzle. An external reservoir containing the THF is placed before the nozzle. The chirp is generated with an arbitrary waveform generator and amplified in a 300W traveling wave tube amplifier before being broadcast intro the vacuum chamber using a horn antenna. Upon chirped microwave excitation we record the free induction decay (FID) of the macroscopic dipole moment of the ensemble of molecules. Using the "fast-frame" option of the digital oscilloscope we excite each gas pulse with eight back-to-back excitation chirps. Eight FID acquisitions are co-added and averaged to obtain the final spectrum. This scheme results in an effective repetition rate of 72 Hz. 500k FIDs were co-added and averaged to produce the final spectrum.

Because of the direct correspondence between unique moments of inertia and molecular structure, molecular complexes can be differentiated from their rotational spectrum and directly compared with theoretical structure predictions. The primary rotational constants (A, B, C) and quartic centrifugal distortion constants were determined through a recurrent fit using the A-reduced semi rigid rotor Hamiltonian as implemented in PGOPHER.[16]

Synthesis of and characterization of 1

A two-necked 100 ml round bottom flask equipped with a condenser and a magnetic stirrer bar was successively charged with malononitrile (1.982 g, 30 mmol), ethanol (20 mL), NaOAc (0.246 g, 3 mmol) and acetone (0.734 mL, 10 mmol). The mixture was magnetically stirred for 30 minutes, resulting in a clear yellow solution. Using a dropping funnel, 50 mL of a 0.2 M bromine solution (10 mmol) in water was added in a dropwise fashion, leading to an yellow/orange suspension. After this mixture was stirred overnight at 40 °C, it was allowed to cool to laboratory temperature resulting in a brown solution with white precipitate. Büchner filtration with water revealed a brown solid which turned white upon an ice-cold ethanol wash (~50 mL). The crude was recrystallized from refluxing ethanol, isolated by filtration over a Hirsch filter and washed with water. Freeze-drying gave 1.42 g (83% yield) of a fluffy white crystalline material analysed as **1**. (see also Figures S1 – Figure S2 for spectra). **Note:** we found that the yield can be greatly impacted by ethanol wash and care should be taken to use thoroughly cooled ethanol throughout the washing.

NMR (see also Figure S1): **^{1}H-NMR** (500 MHz; $CDCl_3$) δ 1.815 (s, 6H, CH_3) p.p.m.; **^{13}C-NMR** (126 MHz; $CDCl_3$) δ 107.908 (s, CN), 40.797 (s, $\underline{C}(CN)_2$), 25.751 (s, $\underline{C}(CH_3)_2$), 20.050 (s, CH_3) p.p.m.; **^{1}H-^{13}C-HSQC-NMR** ($CDCl_3$) δ [1.82 ; 20.05] ($C\underline{H}_3$; $\underline{C}H_3$) p.p.m.; **^{1}H-^{13}C-HMBC-NMR** ($CDCl_3$) δ [1.82 ; 20.05] ($C\underline{H}_3$; $\underline{C}H_3$); [1.82 ; 25.75] ($C\underline{H}_3$; $\underline{C}(CH_3)_2$); [1.82 ; 40.80] ($C\underline{H}_3$; $\underline{C}(CN)_2$) p.p.m.; **FT-IR** (neat, main peaks, see also Figure S2) *v* 2 3396-2978 (small, CH rock and stretch); 223, 2195 (medium, C≡N stretch); 1653, 1602, 1569, 1559 (medium, CH rock); 1395, 1373 (small, C-$C^{cyclopropane}$ stretch); 1174 (medium, C-$C^{cyclopropan}$ rocking); 927, 702, 681 (small, $^{(CN)2}$C-$C^{(CN)2}$ rocking) cm^{-1}; **Elem. anal.** for $C_9H_6N_4$: Found (calc.): C 3.19 (63.52), N 32.85 (32.92), H 3.47 (3.55); **FD-MS** for $[C_9H_6N_4]$+: Found (calc.): 170.0532 (170.0592). **SC-XRD** of $C_{13}H_{14}N_4O$, Mw = 242.28, colourless block, 0.58×0.304×0.244 mm, tetragonal, $P4_12_12$ (No: 92), a = 7.7490(3), b = 7.7490(3), c = 22.0320(11) Å, α = 90, β = 90, γ = 90 °, V = 1322.96(12) Å³, Z = 4, D_x = 1.216 g/cm³, μ = 0.081 mm^{-1}. 63886 Reflections were measured up to a resolution of $(\sin\theta/\lambda)_{max}$ = 0.74 $Å^{-1}$. 1719 Reflections were unique (R_{int} = 0.0542), of which 1576 were observed [I>2σ(I)]. 84 Parameters were refined with 0 restraints. R1/wR2 [I>2σ(I)]: 0.0409/0.1126. R1/wR2 [all refl.]: 0.0468/0.1171. S = 0.975. Residual electron density between 0.168 and -0.225. The flack parameter refined to -0.3(4). CCDC 1983293.

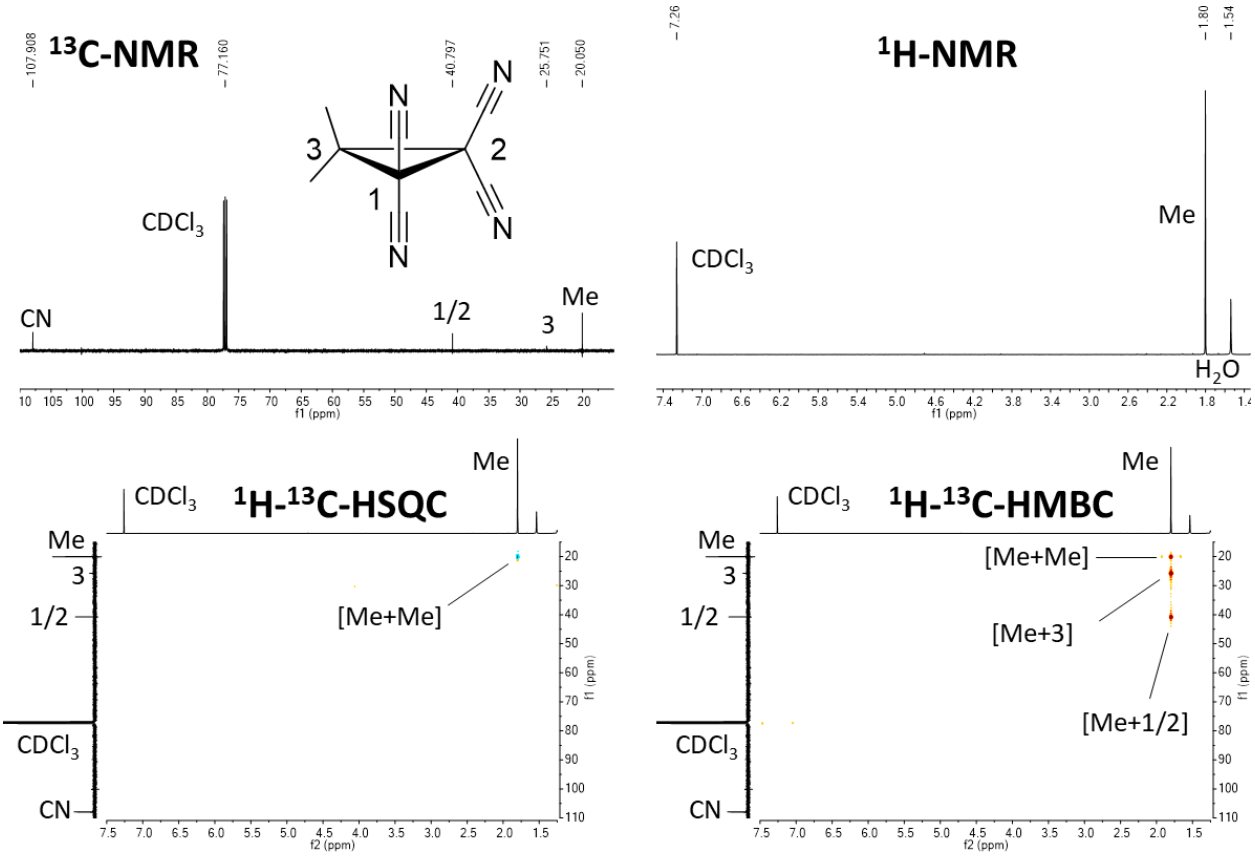

Figure S1. NMR spectra of **1** in $CDCl_3$ solution, together with an assignment of the peaks.

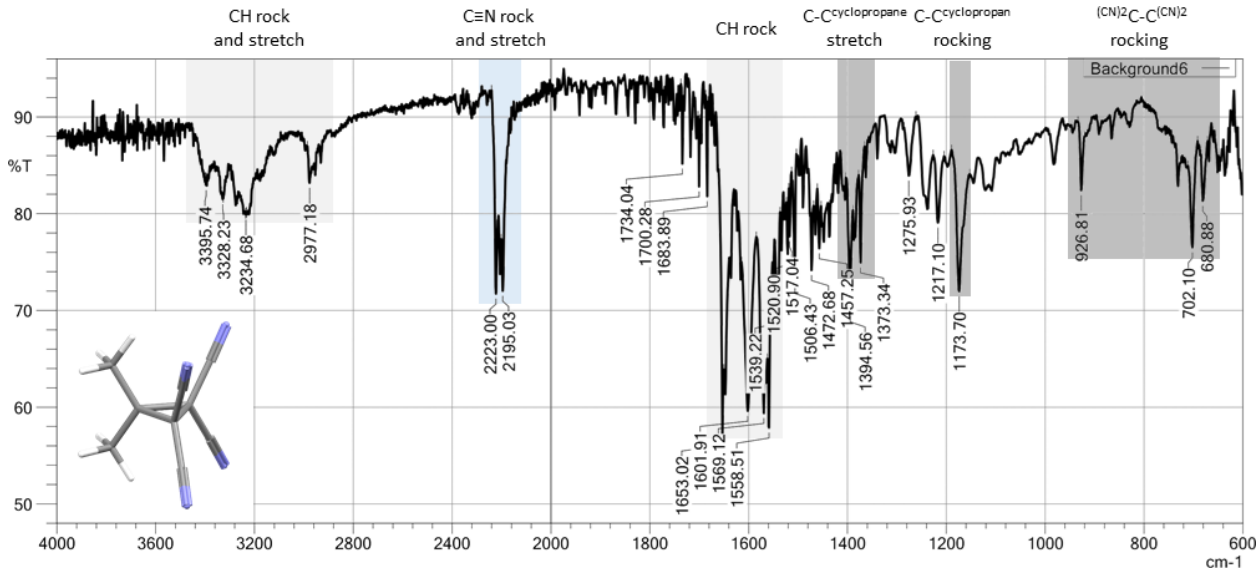

Figure S2. FT-IR spectrum of **1** (neat) together with an assignment of the main peaks. The assignment was aided by the calculated FT-IR spectrum of **1** at the GGA (BLYP-D3(BJ)) / TZ2P level of theory (scalar relativity and no frozen cores) level of theory using ADF.[9]

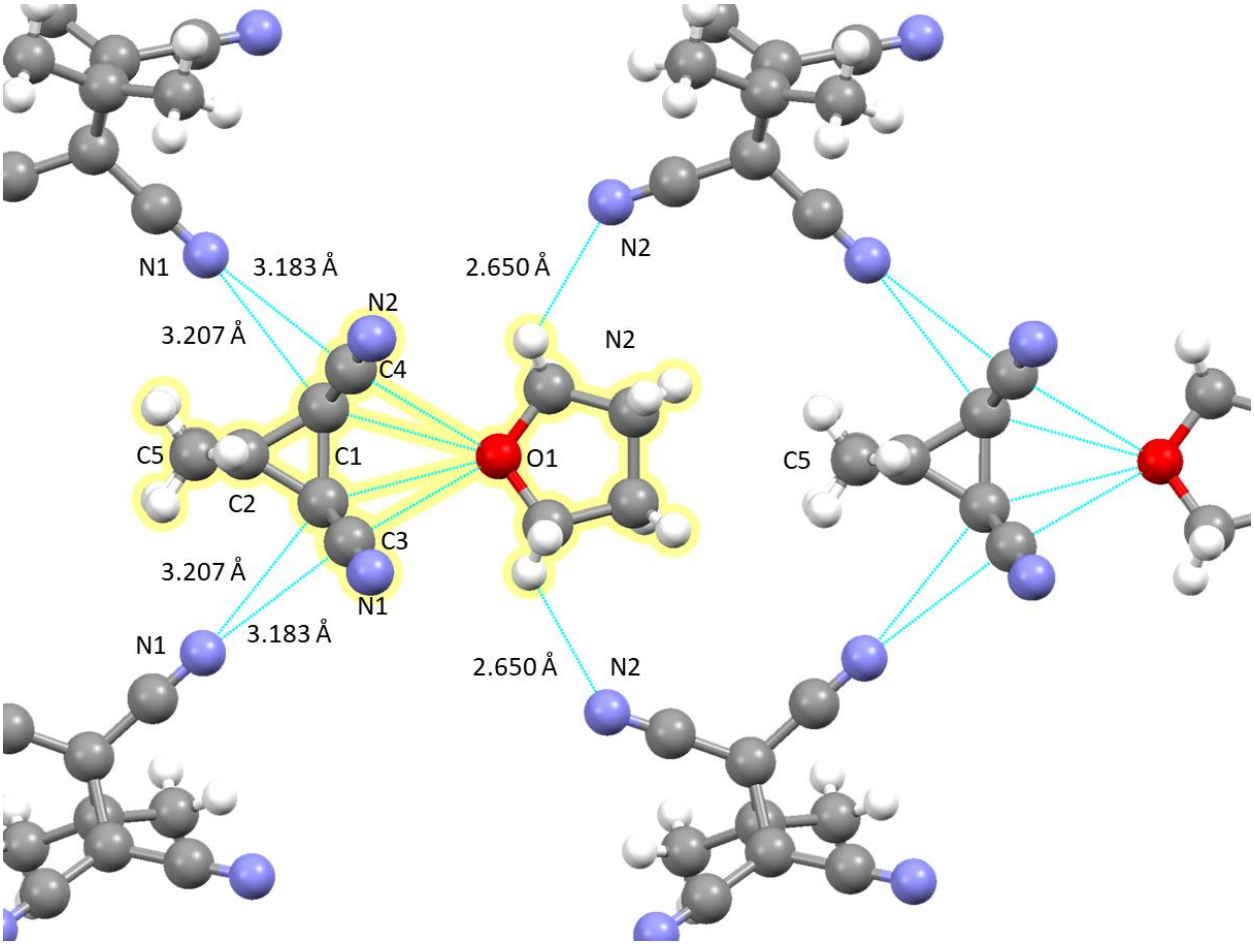

Figure S3. Illustration of other intermolecular (packing) forces around a single [**1**···THF] adduct (highlighted in yellow, see also Figure 1, left) in its crystal structure. The broken cyan lines indicate contact distances found in Mercury 3.8 (Build RC2). Using the typical van der Waals radius of H (1.09 Å), N (1.55 Å) and C (1.70 Å) however, the contacts involving N2 are actually slightly longer than the sum of the van der Waals radii of H + N (2.650–1.09–1.55 = 0.01 Å), leaving the N1···C1(sp^3) and N1···C3(*sp*) interactions as the only other interaction with clearly overlapping van der Waals shells. This overlap is 0.043 Å for N1···C1(3.207–1.70–1.55) and 0.067 Å for N1···C3(3.183–1.70–1.55).

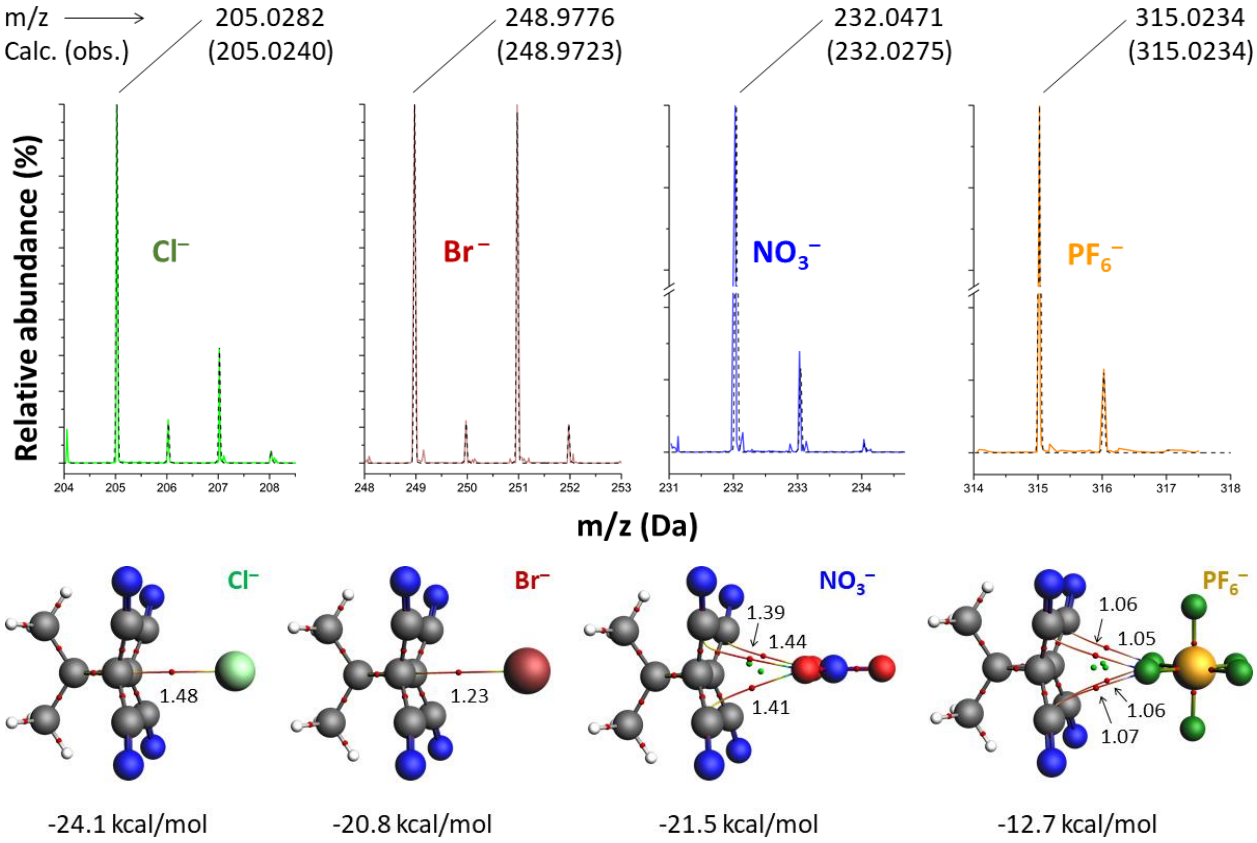

Figure S4. Top: CryoSpray Ionization High Resolution Mass Spectra (CSI HRMS) of anionic adduct of **1** (solid colored lines) together with simulated distributions (dashed black lines). Stock solutions (0.5 mM) of **1** and *n*-butylammonium salts (Cl^-, Br^-, NO_3^-, PF_6^-) were prepared in ultra-pure CH_2Cl_2. Approximately 50 μL the stock solution of **1** and of a salt were diluted to about 2 mL in a 2 mL vial using ultra-pure CH_2Cl_2. The resulting solution thus contained an equimolar amount of **1** and an *n*-butylammonium salt at about 12.5 μM and were used in the measurements. The simulated distributions were were generated by an online tool, available at http://www.chemcalc.org/ and using a Peak Full Width at Half-Maximum (FWHM) of 0.038. Bottom: Geometry optimized (B3LYP-D3/def2-TZVP) adducts of **1** with indicted interaction energies. In each case an 'atoms-in-molecules' analysis was performed at the B3LYP/def2-TZVP level of theory, revealing intermolecular 'bond critical points' (bcp, small red spheres) on their 'bond paths' (bp, thin red lines). The density of these bcp's (ρ) is given in a.u. x 100.

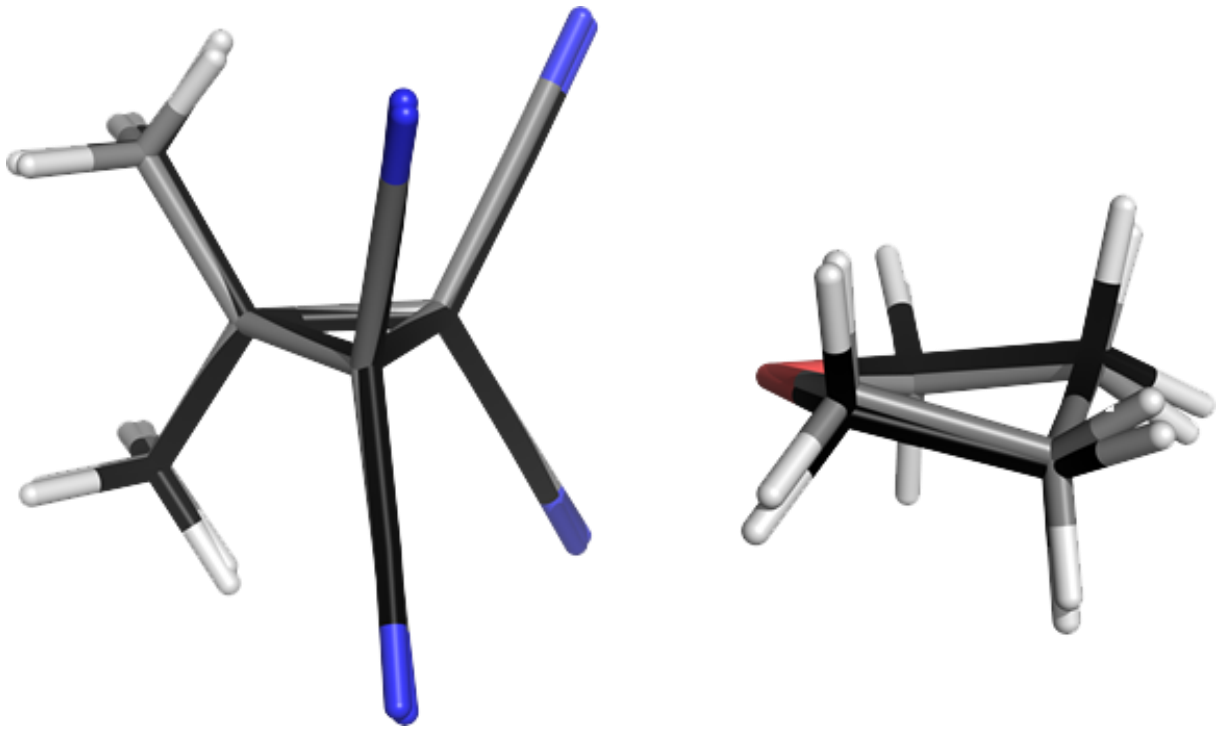

Figure S5. Capped sticks representations of structural overlays (PyMOL, RMDS = 0.161 Å with 32 atoms) of atomic coordinated of the X-ray structure of [**1**···THF] (black sticks) and a geometry optimized structure of [**1**···THF] (grey sticks). The geometry optimizations were done at the B3LYP-D3/def2-TZVP level of theory.

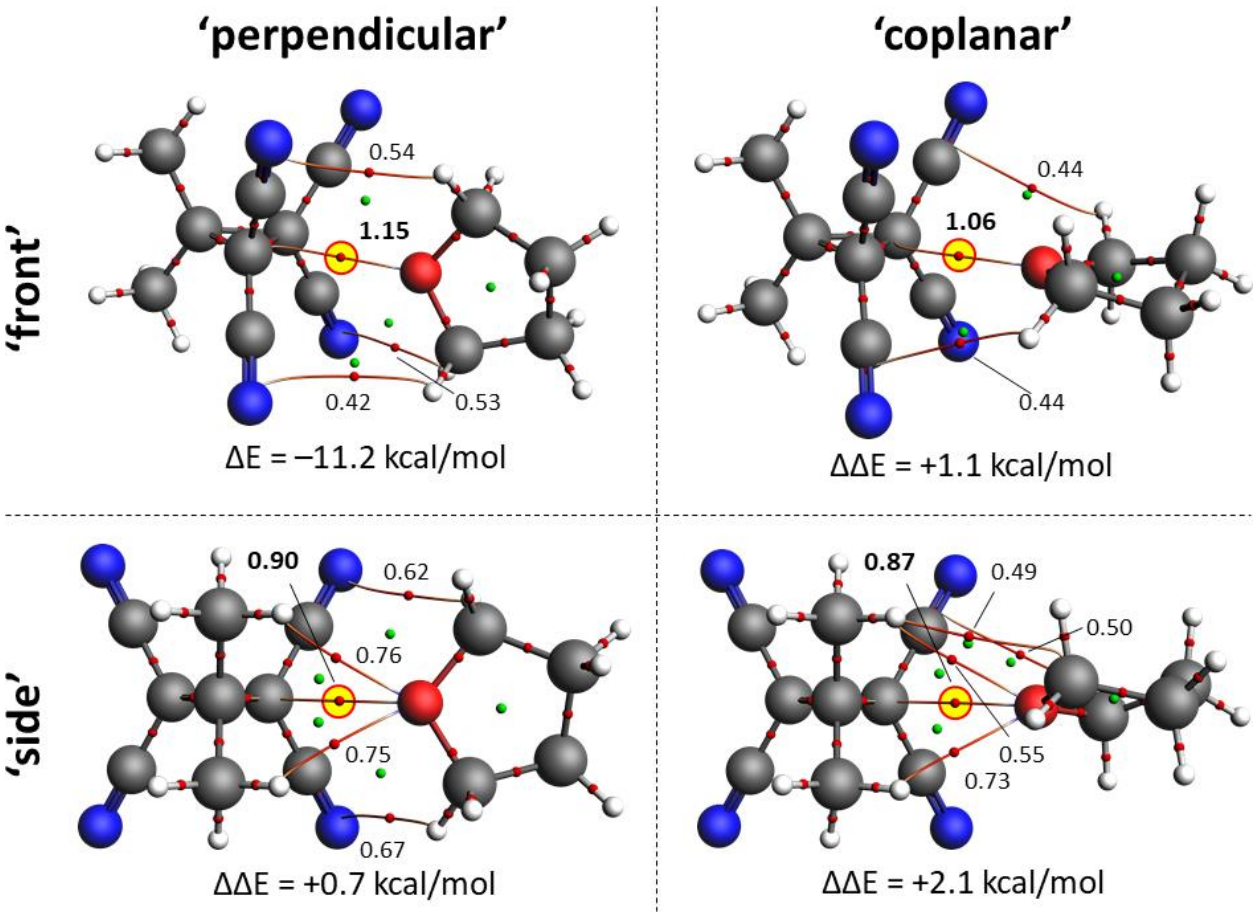

Figure S6. Ball-and stick representations of geometry optimized structures for all four orientations of [**1**···THF] that were calculated at the B3LYP-D3/def2-TZVP level of theory. These orientations are distinguished in the positioning of the THF molecule relative to **1** in two manners: the THF O-atom can be situated at the colloquial 'front' (in between the four CN-groups) or 'side' (in between two CN-groups and two methyl-groups) of **1**; the ring-planes of THF and the cyclopropane core of **1** can be oriented either 'perpendicular' or 'coplanar' relative to one another. The interaction energy (ΔE) of the most stable structure (top left; also measured with rotational IR) is given, together with the energies relative to this structure (ΔΔE) of the other orientations. The interaction energy of these complexes can be decomposed in pauli repulsion (PR), orbital interactions (OI), electrostatic interactions (EI) and dispersive interactions (DI). These were (in kcal/mol): front/perpendicular: +12.43 (PR), –3.96 (OI), –12.44 (EI), –7.19 (DI); front/coplanar: +10.32 (PR), –3.21 (OI), –10.28 (EI), –6.88 (DI); side/perpendicular: +10.11 (PR), –3.45 (OI), –10.48 (EI), –6.78 (DI); side/coplanar: +8.79 (PR), –2.99 (OI), –8.53 (EI), –6.50 (DI). In each case an 'atoms-in-molecules' analysis was performed at the B3LYP/def2-TZVP level of theory, revealing several intermolecular 'bond critical points' (bcp, small red spheres) on their 'bond paths' (bp, thin red lines). The density of these bcp's (ρ) is given in a.u. x 100. There always seem to be several weak C–H···N/O hydrogen bonding interactions with (ρ = 0.4 - 0.7). Interestingly, in all cases the densest bcp is found between the O-atom of THF and an sp^3 C-atom of the cyclopropane core in **1** (also highlighted in yellow).

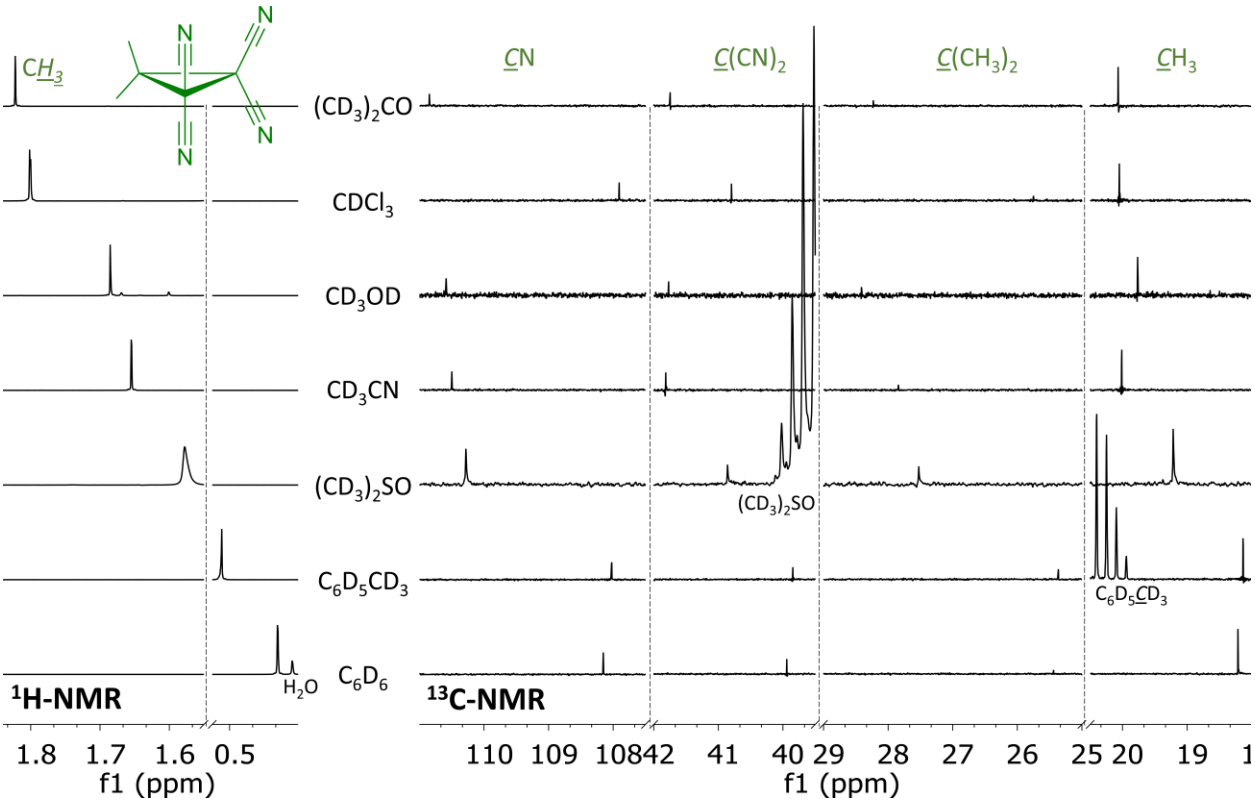

Figure S7. Selected sections of the ^{1}H-(left) and ^{13}C-NMR (right) spectra of **1** in various solvents (as indicated). The maximum difference in chemical shift value of the methyl resonance within this list of solvents ($\Delta\delta_{max}$) is: 1.39 (C*H*$_3$), 1.93 (*C*H$_3$), 3.57 (*C*(Me)$_2$), 2.44 (*C*(CN)$_2$), and 3.12 (*C*N) p.p.m.. See also Table S4 for a numerical comparison of ^{1}H and ^{13}C NMR resonances with those of other methyl groups.

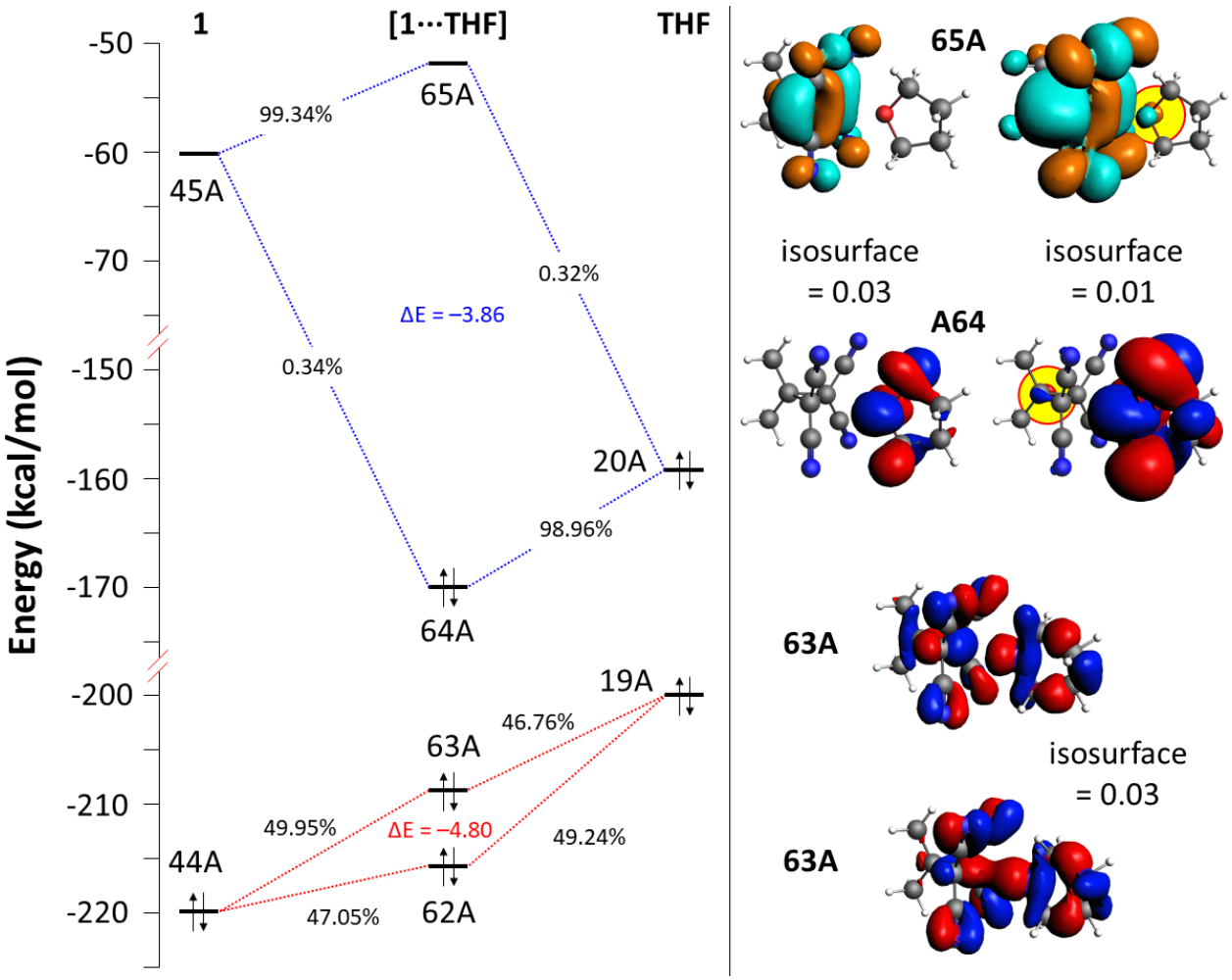

Figure S8. Orbital analysis of the energy minimum [**1**···THF] adduct calculated at the B3LYP-D3/TZ2P level of theory. Left: energy diagram wherein the HOMO(THF)···LUMO(**1**) interaction is indicated in blue dotted lines and the HOMO-(**1**)···HOMO(THF) interactions is indicated in red dotted lines. See Table S1 for the numerical values of the energies of the orbitals involved. Right: ball-and-stick representation of [**1**···THF] with indicated orbitals at 0.03 or 0.01 isosurface. Unoccupied orbitals are in orange-cyan and occupied orbitals are shown in red-blue. The yellow highlight was added as a guide to the eye, indicating that the HOMO(64A) and the LUMO(65A) are both somewhat located on both **1** and THF (only visable when plotted at 0.01 isosurface).

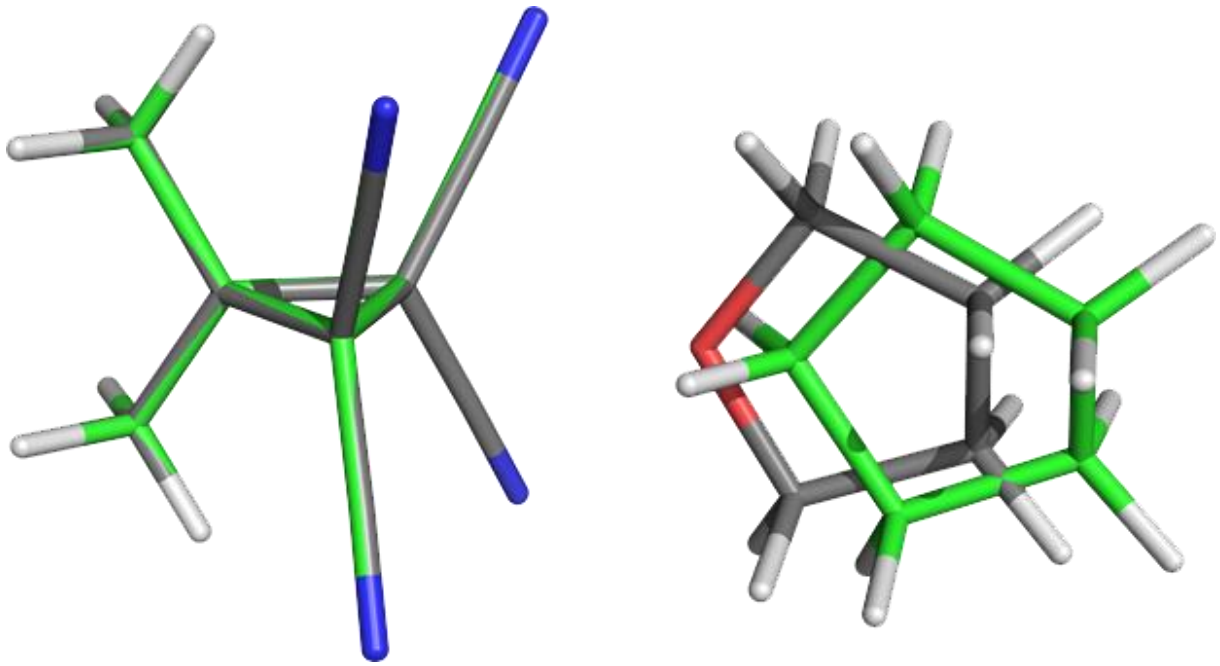

Figure S9. Shown in green sticks is the energy minimized structure of [**1**···cyclopenatane], which was pair-fitted in PyMOL on the heavy atoms of **1** in [**1**···THF]. The geometry optimizations were done at the B3LYP-D3/def2-TZVP level of theory.

Table S1. Numerical overview of the energies of the orbitals shown in Figure S7, together with the energy differences of the hybridization.

Origin	Orbital:	E in kcal/mol	ΔE in kcal/mol
1	45A (LUMO)	–60.245	
1	44A (HOMO)	–219.06	
THF	20A (HOMO)	–158.191	
THF	19A (HOMO-1)	–200.543	
[**1**···THF]	65A (LUMO)	–52.619	–3.86
[**1**···THF]	64A (HOMO)	–169.673	(65A+65A – 20A-45A)
[**1**···THF]	63A (HOMO-1)	–208.492	–4.80
[**1**···THF]	62A (HOMO-2)	–215.914	(62A+63A – 19A-44A)

Table S2. Cartesian coordinates of indicated charge-neutral adducts of **1** resulting from a geometry optimization at the B3LYP-D3 / def2-TZVP level of theory. See also Figures 1, 2, S5, S6 and S8.

Adducts [1···THF]													[1···cyclopentane]		
'front – perpendicular'[a]			'front – coplanar'[b]			'side – perpendicular'			'front – coplanar'						
C	-2.2201	-3.1318	0.3878	C	-0.1090	-0.7570	3.8018	C	1.6938	-0.4105	-3.0885	C	-1.3133	-2.6147	-2.2329	C	-1.3116	-0.0442	1.3251
C	-0.8447	-2.4921	0.2230	C	-0.6260	-0.9911	2.3859	C	1.8428	-0.3112	-1.5771	C	-0.9089	-1.1723	-1.9507	C	-2.5346	0.4451	3.3874
C	-3.0923	-2.2405	-0.5029	C	0.1059	0.7602	3.8090	C	1.0351	0.9324	-3.4203	C	-1.8728	-3.0434	-0.8723	C	-1.1141	0.2509	2.8343
C	-2.4895	-0.8621	-0.2528	C	0.6265	1.0085	2.3963	C	0.1083	1.1474	-2.2212	C	-0.9336	-2.3322	0.0992	C	-3.3740	-0.5274	2.5517
C	1.2022	-0.0169	1.6816	C	1.7212	0.7550	-0.8628	C	-1.0582	-1.8371	3.2956	C	2.5082	2.1722	2.2201	C	-2.8212	-0.3405	1.1301
C	1.8307	1.8432	0.0268	C	0.0003	-0.0017	-2.6156	C	-0.4460	0.1472	1.7838	C	0.8807	1.5919	0.3131	C	1.5341	1.6769	-0.2536
C	0.7765	1.0256	0.7841	C	0.3477	0.6950	-1.2925	C	-1.4966	-0.7675	2.4366	C	1.1620	2.1781	1.7090	C	2.1259	0.0389	-2.1412
C	-0.4655	1.6437	1.1708	C	-0.4400	1.8224	-0.8633	C	-2.7815	-0.2236	2.7927	C	0.3654	3.2825	2.1789	C	1.0886	0.8005	-1.3065
C	1.5363	3.3022	-0.2370	C	-1.1379	0.5708	-3.4271	C	-0.7962	1.6023	1.5831	C	-0.1936	2.2552	-0.5158	C	-0.1455	1.2146	-1.9242
C	-0.0189	1.2335	-1.6477	C	-1.7173	-0.7706	-0.8651	C	-2.1499	-0.4326	-0.0372	C	-0.9567	0.7095	1.8630	C	1.8176	-0.2013	-3.6016
C	1.0165	0.7981	-0.7464	C	-0.3443	-0.7066	-1.2959	C	-1.1519	-0.8771	0.9009	C	0.4426	0.7857	1.5308	C	0.2661	-1.6288	-1.5490
C	1.6348	-0.4414	-1.1408	C	0.4444	-1.8362	-0.8744	C	-0.4344	-2.0459	0.4617	C	1.1869	-0.3932	1.8927	C	1.3118	-0.7444	-1.1032
C	3.2859	1.5400	0.3013	C	1.1358	-0.5703	-3.4339	C	1.0059	-0.0991	2.1186	C	2.0478	1.0568	-0.4822	C	1.9475	-1.1657	0.1192
H	-2.5483	-3.0660	1.4278	H	0.8407	-1.2762	3.9502	H	1.0308	-1.2396	-3.3452	H	-0.4357	-3.2117	-2.4911	C	3.5870	0.2918	-1.8473
H	-2.2298	-4.1811	0.0936	H	-0.8088	-1.1001	4.5637	H	2.6459	-0.5637	-3.5964	H	-2.0350	-2.6975	-3.0453	H	-2.8720	1.4704	3.2049
H	-0.2061	-2.5931	1.1010	H	-0.3685	-1.9743	1.9889	H	1.8672	-1.2773	-1.0744	H	-0.0908	-0.8182	-2.5821	H	-2.6014	0.2650	4.4617
H	-0.3101	-2.8976	-0.6416	H	-1.7116	-0.8631	2.3272	H	2.7447	0.2524	-1.3050	H	-1.7627	-0.4944	-2.0758	H	-0.4662	1.1104	3.0095
H	-2.9744	-2.5209	-1.5523	H	-0.8442	1.2776	3.9602	H	1.7900	1.7204	-3.4702	H	-2.8942	-2.6761	-0.7522	H	-0.6453	-0.6068	3.3223
H	-4.1528	-2.2843	-0.2554	H	0.8037	1.0962	4.5758	H	0.4920	0.9262	-4.3647	H	-1.8805	-4.1233	-0.7281	H	-3.1951	-1.5521	2.8928
H	-2.5798	-0.1831	-1.1009	H	0.3643	1.9934	2.0064	H	0.0280	2.1973	-1.9290	H	-1.4253	-2.0305	1.0249	H	-4.4476	-0.3433	2.6182
H	-2.9310	-0.3800	0.6255	H	1.7128	0.8868	2.3399	H	-0.8976	0.7655	-2.4078	H	-0.0624	-2.9435	0.3496	H	-2.9964	-1.2035	0.4869
H	1.8474	3.8927	0.6255	H	-0.7672	1.3989	-4.0323	H	-0.5550	2.1607	2.4883	H	0.2346	3.1067	-1.0457	H	-3.3095	0.5145	0.6564
H	0.4833	3.4989	-0.4255	H	-1.9564	0.9386	-2.8117	H	-1.8468	1.7635	1.3505	H	-1.0334	2.6082	0.0787	H	2.1294	0.6681	-4.1813
H	2.1079	3.6329	-1.1051	H	-1.5284	-0.1978	-4.0956	H	-0.1939	1.9817	0.7586	H	-0.5671	1.5378	-1.2447	H	0.7625	-0.3822	-3.7944
H	3.8861	1.8573	-0.5522	H	0.7618	-1.3932	-4.0442	H	1.6134	0.2949	1.3051	H	1.6909	0.2357	-1.1027	H	2.3830	-1.0671	-3.9482
H	3.4765	0.4843	0.4808	H	1.9550	-0.9434	-2.8233	H	1.2422	-1.1526	2.2509	H	2.8543	0.6816	0.1444	H	4.1722	-0.5673	-2.1768
H	3.6106	2.1012	1.1784	H	1.5254	0.2025	-4.0974	H	1.2579	0.4286	3.0391	H	2.4453	1.8458	-1.1213	H	3.7900	0.4613	-0.7923
N	1.5702	-0.8298	2.4057	N	2.8257	0.8176	-0.5521	N	-0.6857	-2.6755	3.9882	N	3.5911	2.1715	2.6058	H	3.9174	1.1681	-2.4061
N	-1.4419	2.1633	1.4824	N	-1.0590	2.7409	-0.5576	N	-3.7970	0.2306	3.0819	N	-0.2724	4.1721	2.5298	H	-1.0094	0.8106	0.7191
N	-0.8266	1.6078	-2.3743	N	-2.8212	-0.8371	-0.5530	N	-2.9379	-0.0680	-0.7898	N	-2.0754	0.6428	2.1168	H	-0.7045	-0.8967	1.0185
N	2.1549	-1.4153	-1.4595	N	1.0638	-2.7559	-0.5729	N	0.1522	-2.9711	0.1145	N	1.7781	-1.3384	2.1704	N	1.9082	2.3821	0.5731
O	-1.0879	-1.0883	-0.0017	O	0.0048	0.0102	1.5651	O	0.6786	0.4014	-1.1232	O	-0.4740	-1.1446	-0.5844	N	-1.1167	1.5479	-2.4403
																N	-0.5538	-2.3406	-1.9257
																N	2.4776	-1.5051	1.0806

[a] This orientation corresponds best to the rotational-IR data; [b] this orientation is similar to the X-ray structure.

Table S3. Cartesian coordinates of indicated charge-neutral adducts of **1** resulting from a geometry optimization at the B3LYP-D3 / def2-TZVP level of theory. See also Figure S4.

[1···Cl⁻]⁻				[1···Br⁻]⁻				[1···NO_3^-]⁻				[1···PF_6^-]⁻			
C	-0.0048	0.0007	0.6650	Br	0.0142	-0.0227	-3.8496	C	-1.2074	0.0017	0.0057	C	0.0920	-0.0181	1.7628
C	-0.0120	-1.2681	1.4839	C	-0.0043	0.0008	0.6710	C	-2.0422	0.0010	-1.2539	C	0.1316	-1.2957	2.5689
C	-0.0117	1.2665	1.4885	C	-0.0111	-1.2683	1.4898	C	-2.0238	0.0016	1.2772	C	0.1331	1.2367	2.6039
C	-0.7632	0.0018	-0.6790	C	-0.0112	1.2661	1.4953	C	0.1220	0.7798	-0.0045	C	-0.7496	-0.0008	0.4747
C	0.7764	0.0022	-0.6660	C	-0.7652	0.0022	-0.6713	C	0.1221	-0.7755	-0.0045	C	0.8093	-0.0001	0.4020
C	1.4685	1.2128	-1.0404	C	0.7781	0.0025	-0.6590	C	0.4952	-1.4631	1.2074	C	1.4832	1.2198	0.0300
C	1.4706	-1.2070	-1.0415	C	1.4718	1.2143	-1.0271	C	0.4721	-1.4649	-1.2222	C	1.4844	-1.2090	-0.0016
C	-1.4492	1.2124	-1.0648	C	1.4742	-1.2074	-1.0284	C	0.4907	1.4694	1.2075	C	-1.4566	1.2189	0.1706
C	-1.4507	-1.2076	-1.0660	C	-1.4532	1.2139	-1.0501	C	0.4764	1.4675	-1.2217	C	-1.4573	-1.2120	0.1389
Cl	0.0165	-0.0194	-3.6418	C	-1.4554	-1.2081	-1.0510	H	-2.6827	0.8849	-1.2641	F	-1.2971	0.0303	-2.3345
H	-0.9024	-1.2881	2.1156	H	-0.9014	-1.2877	2.1214	H	-2.6604	0.8881	1.2991	F	-0.1943	1.6520	-3.5287
H	-0.9030	1.2850	2.1191	H	-0.9024	1.2834	2.1259	H	-1.4435	0.0044	-2.1606	F	0.9120	0.0358	-4.7369
H	-0.0097	-2.1660	0.8717	H	-0.0087	-2.1666	0.8784	H	-1.4125	-0.0004	2.1755	F	-1.3978	0.0355	-4.6407
H	-0.0073	2.1669	0.8798	H	-0.0066	2.1674	0.8882	H	-2.6621	-0.8839	1.2965	F	1.0044	0.0300	-2.4299
H	0.8694	1.2856	2.1331	H	0.8698	1.2838	2.1399	H	-2.6768	-0.8872	-1.2675	F	-0.1941	-1.5861	-3.5366
H	0.8701	-1.2914	2.1270	H	0.8710	-1.2906	2.1327	N	0.6282	-2.0269	2.2004	H	-0.7268	-1.3245	3.2422
N	2.0651	2.1892	-1.1571	N	2.0665	2.1924	-1.1384	N	0.5808	-2.0322	-2.2163	H	-0.7245	1.2473	3.2789
N	2.0707	-2.1818	-1.1542	N	2.0728	-2.1836	-1.1361	N	0.6173	2.0365	2.1996	H	0.1105	-2.1901	1.9521
N	-2.0441	2.1891	-1.1877	N	-2.0461	2.1925	-1.1675	N	0.5945	2.0322	-2.2162	H	0.1121	2.1478	2.0120
N	-2.0491	-2.1828	-1.1853	N	-2.0527	-2.1845	-1.1642	N	3.5632	-0.0081	-0.0089	H	1.0456	1.2389	3.2026
								O	2.9284	1.0831	-0.0052	H	1.0433	-1.3156	3.1683
								O	4.7999	-0.0138	0.0310	N	2.0482	2.2071	-0.1309
								O	2.9207	-1.0942	-0.0543	N	2.0505	-2.1915	-0.1867
												N	-2.0323	2.2079	0.0679
												N	-2.0336	-2.1976	0.0108
												P	-0.1960	0.0331	-3.5603

Table S4. Comparison of selected NMR chemical shifts of the methyl groups in **1** (γ-protons) and the methyl groups in hexane (non-acidic) and the β-protons of Et_2O and EtOAc as taken from reference 17.

	^{1}H NMR δ in p.p.m. of C<u>*H*</u>$_3$ in:				^{13}C NMR δ in p.p.m. of <u>*C*</u>H$_3$ in:			
	1	Hexane	Et_2O	EtOAc	**1**	Hexane	Et_2O	EtOAc
$(CD_3)_2CO$	1.82	0.86	1.11	1.20	20.07	14.34	15.78	14.50
$CDCl_3$	1.80	0.88	1.21	1.26	20.05	14.14	15.20	14.19
CD_3OD	1.69	0.90	1.18	1.24	19.77	14.45	15.46	14.49
CD_3CN	1.65	0.89	1.12	1.20	20.01	14.43	15.63	14.54
$(CD_3)_2SO$	1.58	0.86	1.09	1.17	19.22	13.88	15.12	14.40
C_6D_5-CD_3	0.51	0.88	1.10	0.94	18.13	14.34	15.47	14.23
C_6D_6	0.43	0.89	1.11	0.92	18.21	14.32	15.46	14.19
$\Delta\delta_{max}$ [a]	**1.39**	0.04	0.12	0.34	**1.93** [b]	0.57	0.66	0.35

[a] Maximum difference in chemical shift value of the methyl resonance within the given list of solvents; [b] $\Delta\delta_{max}$ for the other ^{13}C NMR resonances of **1** are: 3.12 (<u>*C*</u>N), 2.44 (<u>*C*</u>$(CN)_2$), 3.57 (<u>*C*</u>$(Me)_2$) p.p.m.. See also Figure S7.

References:

1. Bruker, *APEX2 software*, USA, Madison WI, 2014.
2. G. M. Sheldrick, *SADABS*, Germany, Universität Göttingen, 2008.
3. G. M. Sheldrick, *SHELXL2013*, Germany, Universität Göttingen, 2013.
4. A. D. Becke, *Phys. Rev. A*, 1988, **38**, 3098-3100.
5. C. T. Lee, W. T. Yang and R. G. Parr, *Phys. Rev. B*, 1988, **37**, 785-789.
6. S. Grimme, J. Antony, S. Ehrlich and H. Krieg, *J. Chem. Phys.*, 2010, **132**, Art. Nr: 154104.
7. F. Weigend and R. Ahlrichs, *Phys. Chem. Chem. Phys.*, 2005, **7**, 3297-3305.
8. F. Weigend, *Phys. Chem. Chem. Phys.*, 2006, **8**, 1057-1065.
9. G. te Velde, F. M. Bickelhaupt, E. J. Baerends, C. F. Guerra, S. J. A. van Gisbergen, J. G. Snijders and T. Ziegler, *J. Comput. Chem.*, 2001, **22**, 931-967.
10. R. F. W. Bader, *Acc. Chem. Res.*, 1985, **18**, 9-15.
11. F. M. Bickelhaupt and E. J. Baerends, in *Reviews in Computational Chemistry, Vol 15*, eds. K. B. Lipkowitz and D. B. Boyd, Wiley-Vch, Inc, New York, 2000, vol. 15, pp. 1-86.
12. S. C. C. van der Lubbe and C. F. Guerra, *Chem. Asian J.*, 2019, **14**, 2760-2769.
13. T. J. Mooibroek, *Molecules*, 2019, **24**, At. Nr: 3370.
14. D. Schmitz, V. A. Shubert, T. Betz and M. Schnell, *J. Mol. Spectrosc.*, 2012, **280**, 77-84.
15. C. Perez, S. Lobsiger, N. A. Seifert, D. P. Zaleski, B. Temelso, G. C. Shields, Z. Kisiel and B. H. Pate, *Chem. Phys. Lett.*, 2013, **571**, 1-15.
16. C. M. Western, *J. Quant. Spectrosc. Radiat. Transf.*, 2017, **186**, 221-242.
17. G. R. Fulmer, A. J. M. Miller, N. H. Sherden, H. E. Gottlieb, A. Nudelman, B. M. Stoltz, J. E. Bercaw and K. I. Goldberg, *Organometallics*, 2010, **29**, 2176-2179.